

# Mueller matrix approach for determination of optical rotation in chiral turbid media in backscattering geometry

S. Manhas<sup>1</sup>, M. K. Swami<sup>2</sup>, P. Buddhiwant<sup>1</sup>, N. Ghosh<sup>1\*</sup>, P. K. Gupta<sup>1</sup> and K. Singh<sup>2</sup>

<sup>1</sup> Biomedical Applications Section,

Center for Advanced Technology, Indore, India –452013.

<sup>2</sup> Department of Physics, Indian Institute of Technology, Delhi, India

[neem@cat.ernet.in](mailto:neem@cat.ernet.in)

**Abstract:** For in vivo determination of optically active (chiral) substances in turbid media, like for example glucose in human tissue, the backscattering geometry is particularly convenient. However, recent polarimetric measurements performed in the backscattering geometry have shown that, in this geometry, the relatively small rotation of the polarization vector arising due to the optical activity of the medium is totally swamped by the much larger changes in the orientation angle of the polarization vector due to scattering. We show that the change in the orientation angle of the polarization vector arises due to the combined effect of linear diattenuation and linear retardance of light scattered at large angles and can be decoupled from the pure optical rotation component using polar decomposition of Mueller matrix. For this purpose, the method developed earlier for polar decomposition of Mueller matrix was extended to incorporate optical rotation in the medium. The validity of this approach for accurate determination of the degree of optical rotation using the Mueller matrix measured from the medium in both forward and backscattering geometry was tested by conducting studies on chiral turbid samples prepared using known concentration of scatterers and glucose molecules.

© 2006 Optical Society of America

**OCIS Codes:** (170.0170) Medical optics and biotechnology, (170.4580) Optical diagnosis for medicine, (120.5410) Polarimetry, (290.4210) Multiple scattering, (110.7050) Turbid media

## References

1. S.L. Jacques, R.J. Roman and K. Lee, "Imaging skin pathology with polarized light," *J. Biomed. Opt.* **7**, 329 – 340 (2002).
2. S. P. Morgan and I. M. Stockford, "Surface-reflection elimination in polarization imaging of superficial tissue," *Opt. Lett.* **28**, 114-116 (2003).
3. J. M. Schmitt, A. H. Gandjbakhche, and R. F. Bonner, "Use of polarized light to discriminate short path photons in a multiply scattering medium," *Appl. Opt.* **31**, 6535-6546 (1992).
4. V. Backman, R. Gurjar, K. Badizadegan, I. Itzkan, R.R. Dassari, L.T. Perelman, and M.S. Feld, "Polarized light scattering spectroscopy for quantitative measurement of epithelial cellular structure," *IEEE J. Sel. Top. Quantum Electron.* **5**, 1019 – 1026 (1999).
5. M.I. Mischenko, J.W. Hovenier, L.D. Travis, "Light scattering by nonspherical particles" Academic Press, San Diego, 1999.
6. D. Bicut, C. Brosseau, A.S. Martinez, J.M. Schmitt "Depolarization of multiply scattered waves by spherical diffusers :Influence of size parameter," *Phys. Rev. E* **49**, 1767-1770 (1994).
7. V. Sankaran, J. T. Walsh, Jr., and D. J. Maitland, "Comparative study of polarized light propagation in biological tissues," *J. Biomed. Opt.* **7**, 300 – 306 (2002).
8. A.D. Kim, M. Moscoso, "Influence of the refractive index on the depolarization of multiply scattered waves," *Phys. Rev. E* **64**, 026612, 1 –4 (2001).
9. N. Ghosh, P.K. Gupta, H.S. Patel, B. Jain and B.N. Singh, "Depolarization of light in tissue phantoms – effect of collection geometry," *Opt. Commun.* **222**, 93 –100 (2003).

10. N. Ghosh, H.S. Patel, P.K. Gupta, "Depolarization of light in tissue phantoms – effect of a distribution in the size of scatterers," *Opt. Express* **11**, 2198–2205 (2003).  
<http://www.opticsexpress.org/abstract.cfm?URI=OPEX-11-18-2198>
11. N. Ghosh, A. Pradhan, P. K. Gupta, S. Gupta, V. Jaiswal and R. P. Singh, "Depolarization of light in a multiply scattering medium: effect of refractive index of scatterer," *Phys. Rev. E* **70**, 066607 (2004).
12. R. J. McNichols, G.L. Cote, "Optical glucose sensing in biological fluids: an overview," *J. Biomed. Opt.* **5**, 5–16 (2000).
13. B.D.Cameron and G.L. Cote, "Noninvasive glucose sensing utilizing a digital closed loop polarimetric approach," *IEEE Trans. Biomed. Eng.* **44**, 1221–1227 (1997).
14. I.A.Vitkin, E. Hoskinson, "Polarization studies in multiply scattering chiral media," *Opt. Eng.* **39**, 353-362 (2000).
15. K.C.Hadley, I.A. Vitkin, "Optical rotation and linear and circular depolarization rates in diffusively scattered light from chiral, racemic and achiral turbid media," *J. Biomed. Opt.* **7**, 291-299 (2002).
16. I.A. Vitkin, R.D. Laszlo, C.L. Whyman, "Effects of molecular asymmetry of optically active molecules on the polarization properties of multiply scattered light," *Opt. Express* **10**, 222–229 (2002).  
<http://www.opticsexpress.org/abstract.cfm?URI=OPEX-10-4-222>
17. A. Vitkin and R.C.N Studinski, "Polarization preservation in diffusive scattering from in-vivo turbid biological media: Effects of tissue optical absorption in the exact backscattering direction," *Opt. Commun.* **190**, 37–43 (2001).
18. X.Wang, G. Yao and L.V. Yang, "Monte Carlo model and single scattering approx. Of the propagation of polarized light in turbid media containing glucose," *Appl. Opt.* **41**, 792–801, (2002).
19. R.R. Ansari, S. Bockle, and L. Rovati, "New optical scheme for a polarimetric-based glucose sensor," *J. Biomed. Opt.* **9**, 103–115 (2004).
20. M.P.Silverman, W. Strange, J. Badoz, I.A. Vitkin, "Enhanced optical rotation and diminished depolarization in diffusive scattering from a chiral liquid," *Opt. Commun.* **132**, 410-416 (1996).
21. D. Cote and I.A. Vitkin, "Balanced detection for low-noise precision polarimetric measurements of optically active, multiply scattering tissue phantoms," *J. Biomed. Opt.* **9**, 213–220 (2004).
22. Danial Cote and I.A. Vitkin, "Robust concentration determination of optically active molecule in turbid media with validated three dimensional polarization sensitive Monte Carlo calculation," *Opt. Express* **13**, 148–163 (2005). <http://www.opticsexpress.org/abstract.cfm?URI=OPEX-13-1-148>
23. S. Yau Lu and R. A. Chipman, "Interpretation of Mueller matrices based on polar decomposition," *J. Opt. Soc. Am. A* **13**, 1106–1113 (1996).
24. J. Morio and F.Goudail, "Influence of the order of diattenuator, retarder, and polarizer in polar decomposition of Mueller matrices," *Opt. Lett.* **29**, 2234-2236 (2004).
25. C.F. Bohren, D.R. Huffman, "Absorption and scattering of light by small particles," Wiley, New York (1983).
26. R.A.Chipman "Hand book of optics (polarimetry)," OSA / McGraw-Hill, 22.1-22.35, (1994).
27. E. Collette, "Polarized Light: Fundamentals and Applications," Marcel Dekker Inc. New York (1990).
28. Justin S. Baba, J.R. Chung, A.H. DeLaughter, B.D. Cameron, G.L. Cote, "Development and calibration of an automated Mueller matrix polarization imaging system," *J. Biomed. Opt.* **7**, 341–348 (2002).

## 1. Introduction

Studies on polarization properties of scattered light from a turbid medium like human tissue have received considerable attention because the depolarization of scattered light can be used as an effective tool to discriminate against multiply scattered light and thus can facilitate imaging through tissue [1-3]. Further, measurement of polarization properties of scattered light, such as depolarization, retardance and diattenuation, can facilitate quantification of useful physiological and morphological parameters of tissue [4,5]. For example, since the rate of depolarization of incident linearly and circularly polarized light depends on the morphological parameters like the density, size, distribution, shape and refractive index of scatterers present in the medium [6-11], this information may be used for quantitative tissue diagnosis. Similarly, it is well known that the presence of asymmetric chiral molecules like glucose leads to rotation of the plane of linearly polarized light about the axis of propagation. Motivated by the fact that measurement of optical rotation might turn out to be an attractive approach for non-invasive monitoring of glucose level in human tissue, several studies have addressed measurement of polarization properties of light scattered from chiral turbid medium [12 -18]. A major problem in determining the concentration of chiral substances in a turbid medium, is the fact that unlike dilute solutions, the incident polarized light gets strongly depolarized due to multiple scattering and only a small fraction of the light coming out from

the medium retains its initial state of polarization [15,17]. Techniques such as polarization modulation and synchronous detection methods have therefore been developed to extract the surviving polarization fraction of polarized light scattered from chiral turbid medium and analyze this for quantification of the degree of optical rotation [19 -21]. However, recent studies [22] based on this approach have shown that in the backscattering geometry, the relatively small rotation of the polarization vector arising due to the optical activity of the medium is totally swamped by the much larger changes in the orientation angle of the polarization vector due to scattering. In contrast, this effect was observed to be minimal in the forward scattering direction. Based on this observation, it was proposed that in order to avoid errors in concentration determination of chiral molecules in turbid samples, the scattered light in the forward direction should be used [22].

In this communication, we show that the change in the orientation angle of the polarization vector of light propagating through a chiral turbid medium arises not only due to the circular retardance property of the medium (introduced by the presence of chiral molecules) but also is contributed by linear diattenuation (different attenuation of two orthogonal linear polarization) and linear retardance (dephasing of two orthogonal linear polarization) of light scattered at large angles. We present a method based on polar-decomposition of Mueller matrix that can decouple the contribution of linear diattenuation and linear retardance and extract the contribution of optical rotation purely due to the circular retardance property of the medium using the Mueller matrix measured from the medium in both forward and backscattering geometry. This method is an extension of the previously developed method for polar decomposition of Mueller matrix [23] and incorporates the optical rotation matrix in the decomposition process. The validity of this approach was tested by conducting studies on chiral turbid samples prepared using known concentration of scatterers and glucose molecules.

## 2. Theory

### 2.1 Polar decomposition process for separating out linear retardance and circular retardance:

The process for Polar decomposition of experimentally measured Mueller matrix into Mueller matrices of a diattenuator  $\mathbf{M}_D$  (component that causes different amplitude changes for its orthogonal eigen states), a retarder  $\mathbf{M}_R$  (component that causes dephasing of two eigen states) and a depolarizer  $\mathbf{M}_A$  (component that causes depolarization) has been described in details by Lu and Chipman [23]. Here, we discuss this in brief.

Mueller matrix of any sample can be decomposed in the form

$$\mathbf{M} = \mathbf{M}_A \mathbf{M}_R \mathbf{M}_D \quad (1)$$

The diattenuation matrix  $\mathbf{M}_D$  is defined as

$$\mathbf{M}_D = \begin{pmatrix} 1 & \bar{\mathbf{D}}^T \\ \bar{\mathbf{D}} & m_D \end{pmatrix} \quad (2)$$

where

$$m_D = \sqrt{1 - D^2} \mathbf{I} + (1 - \sqrt{1 - D^2}) \hat{\mathbf{D}} \hat{\mathbf{D}}^T \quad (3)$$

$\mathbf{I}$  is 3X3 identity matrix,  $\bar{\mathbf{D}}$  is diattenuation vector and  $\hat{\mathbf{D}}$  is its unit vector and are defined as

$$\vec{D} = \frac{1}{m_{00}} [m_{01} \quad m_{02} \quad m_{03}]^T, \quad \hat{D} = \frac{\vec{D}}{|\vec{D}|} \quad (4)$$

$m_{ij}$  is matrix element of  $i^{\text{th}}$  row and  $j^{\text{th}}$  column of Mueller matrix  $\mathbf{M}$ .

The product of the retardance and the depolarizing matrices can then be obtained as,

$$\mathbf{M}_\Delta \mathbf{M}_R = \mathbf{M}' = \mathbf{M} \mathbf{M}_D^{-1} \quad (5)$$

The matrices  $\mathbf{M}_\Delta$ ,  $\mathbf{M}_R$  and  $\mathbf{M}'$  have the following form

$$\begin{aligned} \mathbf{M}_\Delta &= \begin{pmatrix} 1 & \vec{0} \\ \vec{P}_\Delta & m_\Delta \end{pmatrix} \\ \mathbf{M}_R &= \begin{pmatrix} 1 & \vec{0} \\ \vec{0} & m_R \end{pmatrix} \\ \mathbf{M}' &= \begin{pmatrix} 1 & \vec{0} \\ \vec{P}_\Delta & m' \end{pmatrix} \end{aligned} \quad (6)$$

Here,  $\vec{P}_\Delta = \frac{\vec{P} - m\vec{D}}{1 - D^2}$ , Polarizance vector  $\vec{P} = \frac{1}{m_{00}} [m_{10} \quad m_{20} \quad m_{30}]^T$ , [ $m$  is the sub-matrix of  $\mathbf{M}$ ].

$m'$  is the sub matrix of  $\mathbf{M}'$  and can be written as

$$m' = m_\Delta m_R \quad (7)$$

The sub matrix  $m_\Delta$  can be computed using  $m'$  as

$$m_\Delta = \pm [m'(m')^T + (\sqrt{\lambda_1 \lambda_2} + \sqrt{\lambda_2 \lambda_3} + \sqrt{\lambda_3 \lambda_1}) \mathbf{I}]^{-1} \times [(\sqrt{\lambda_1} + \sqrt{\lambda_2} + \sqrt{\lambda_3}) m'(m')^T + \sqrt{\lambda_1 \lambda_2 \lambda_3} \mathbf{I}] \quad (8)$$

Where  $\lambda_1, \lambda_2$  and  $\lambda_3$  are eigen values of  $m'(m')^T$ . The sign “+” or “-” in the right side of Eq. (8) is determined by the sign of determinant of  $m'$ .

Using Eqs. (7) and (8), the expression for the sub matrix  $m_R$  of the retardance matrix  $\mathbf{M}_R$  can be obtained as

$$m_R = m_\Delta^{-1} m' \quad (9)$$

Using Eqs. (6) and (9), the total retardance matrix  $\mathbf{M}_R$  can be computed.

The decomposed retardance matrix  $\mathbf{M}_R$  can further be used to determine the value of optical rotation. The total retardance ( $R$ ) and the elements of the retardance vector  $\bar{R} = [1, r_1, r_2, r_3]$  can be written as

$$r_i = \frac{1}{2\sin R} \sum_{j,k=1}^3 \epsilon_{ijk} (m_R)_{jk} \quad (10)$$

here  $\epsilon_{ijk}$  is Levi-civita permutation symbol.

$$R = \cos^{-1} \left\{ \frac{\text{tr}(\mathbf{M}_R)}{2} - 1 \right\} \quad (11)$$

The retardance matrix  $\mathbf{M}_R$  can be written as a combination of linear retardance matrix and optical rotation matrix

$$\mathbf{M}_R = \begin{pmatrix} 1 & 0 & 0 & 0 \\ 0 & \cos^2 2\theta + \sin^2 2\theta \cos \delta & \sin 2\theta \cos 2\theta (1 - \cos \delta) & -\sin 2\theta \sin \delta \\ 0 & \sin 2\theta \cos 2\theta (1 - \cos \delta) & \sin^2 2\theta + \cos^2 2\theta \cos \delta & \cos 2\theta \sin \delta \\ 0 & \sin 2\theta \sin \delta & -\cos 2\theta \sin \delta & \cos \delta \end{pmatrix} \times \begin{pmatrix} 1 & 0 & 0 & 0 \\ 0 & \cos 2\psi & \sin 2\psi & 0 \\ 0 & -\sin 2\psi & \cos 2\psi & 0 \\ 0 & 0 & 0 & 1 \end{pmatrix} \quad (12)$$

Here  $\delta$ ,  $\theta$  and  $\psi$  are linear retardance, orientation of fast axis of the linear retarder and optical rotation respectively.

Using Eqs. (11) and (12), the total retardance ( $R$ ) can be expressed as

$$R = \cos^{-1} \left\{ 2\cos^2(\psi)\cos^2\left(\frac{\delta}{2}\right) - 1 \right\} \quad (13)$$

Similarly, the square of the fourth element of the retardance vector ( $r_3^2$ ) can be expressed as

$$r_3^2 = \frac{\sin^2 \psi \cos^2 \left( \frac{\delta}{2} \right)}{1 - \cos^2(\psi) \cos^2 \left( \frac{\delta}{2} \right)} \quad (14)$$

It can be seen from Eqs. (13) and (14) that  $R$  and  $r_3^2$  are function of linear retardance ( $\delta$ ) and optical rotation ( $\psi$ ) and are independent of the orientation of the fast axis of the linear retarder ( $\theta$ ). Therefore, using Eqs. (13) and (14), linear retardance and optical rotation ( $\psi$ ) can be expressed as

$$\delta = 2\cos^{-1} \left\{ \sqrt{r_3^2 \left( 1 - \cos^2(R/2) \right) + \cos^2(R/2)} \right\} \quad (15)$$

$$\psi = \cos^{-1} \left\{ \frac{\cos(R/2)}{\cos(\delta/2)} \right\} \quad (16)$$

The orientation of the fast axis with respect to the horizontal axis ( $\theta$ ) can also be determined using the relationship [23]

$$\theta = \frac{1}{2} \tan^{-1} \left\{ \frac{r_3}{r_2} \right\} \quad (17)$$

It thus, follows that following the process described above, one can obtain values for  $\delta$  and  $\psi$  separately using the total retardance matrix  $\mathbf{M}_R$ . The total polar decomposition process is illustrated in the flow chart shown in Fig. 1.

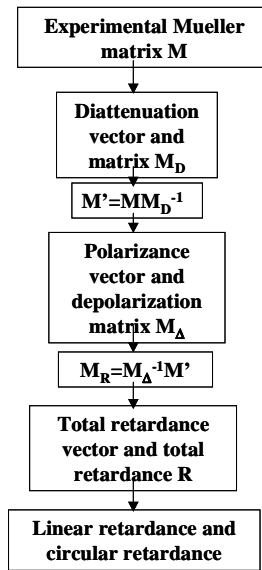


Fig. 1. Flow chart for polar decomposition of an experimentally obtained Mueller Matrix

It should be mentioned here that the decomposition of Mueller matrix also depends upon the order in which the diattenuator, depolarizer and retarder matrices are multiplied. Based on the order of these matrices, six possible decompositions can be performed [24]. These six possible decomposition processes can again be classified in to two groups depending upon the order in which the diattenuator and the depolarizer matrices are multiplied. The group in which the diattenuator matrix comes ahead of the depolarization matrix always leads to a physically realizable Mueller matrix [24]. The decomposition process discussed in this section is therefore based on this convention.

## 2.2 Decomposition of single scattering Mueller matrix:

In order to demonstrate the applicability of the procedure outlined in Section 2.1, for separation of contribution of linear retardance from circular retardance from the total

retardance matrix ( $\mathbf{M}_R$ ), we first consider the case of scattering from spherical scatterers with known size and refractive index.

The scattering matrix  $S(\Theta)$  for a spherical scatterer with diameter  $2.0\ \mu\text{m}$  at a wavelength  $\lambda = 632.8\ \text{nm}$  was computed using Mie theory [25]. The refractive index of the scatterer ( $n$ ) and that of the surrounding medium ( $n_{\text{medium}}$ ) was taken to be  $n = 1.59$  and  $n_{\text{medium}} = 1.33$  respectively. The variation in the value for the orientation angle of the polarization vector ( $\gamma$ ) as a function of scattering angle  $\Theta$  of an incident beam polarized at an angle  $\gamma_0 = 45^\circ$  after single scattering from the scatterer is shown in Fig. 2(a). Here,  $\gamma$  is defined as

$$\gamma = 0.5 \times \tan^{-1} (U / Q) \quad (18)$$

$Q$  and  $U$  are the second and the third element of the Stoke's vector [25].

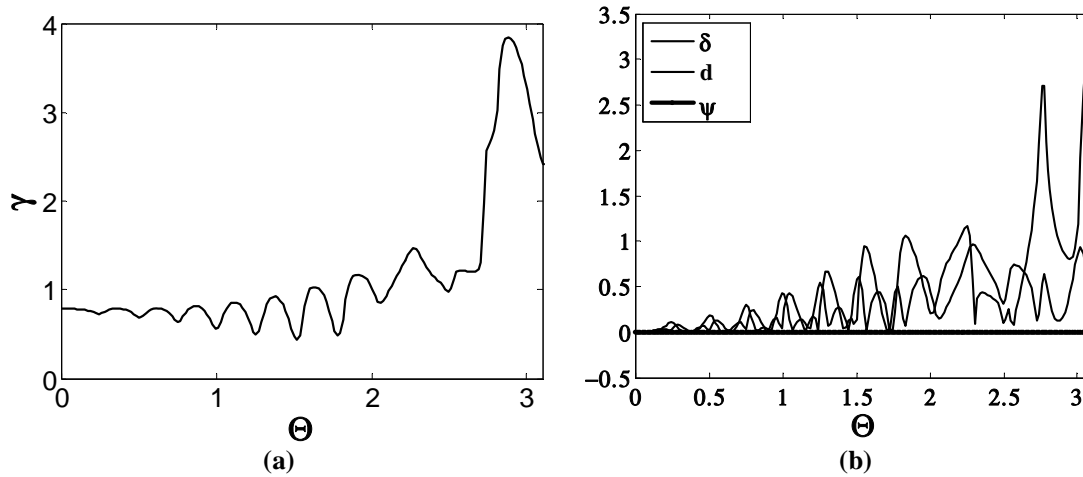


Fig. 2. (a) The variation of the orientation angle ( $\gamma$ ) as a function of scattering angle  $\Theta$ . (b) The values for linear retardance  $\delta$  (solid line), diattenuation  $d$  (dotted line) and optical rotation  $\psi$  (dash dotted line) obtained from polar decomposition of single scattering Mueller matrix ( $\delta$  and  $\psi$  are in radian).

In agreement with the results of Cote *et al* [22],  $\gamma$  is seen to vary considerably as a function of  $\Theta$ , with its value being significantly larger in the backscattering direction ( $\Theta > 1.57$  radian) as compared to that in the forward scattering direction ( $\Theta < 0.523$  radian). The values for the linear diattenuation ( $d$ ) linear retardance ( $\delta$ ) and optical rotation ( $\psi$ ) were calculated following the process described in Section 2.1. The variations of  $d$ ,  $\delta$  and  $\psi$  as a function of  $\Theta$  are displayed in Fig. 2(b). The values for  $d$  and  $\delta$  are observed to vary significantly as a function of  $\Theta$ . However, as can be seen, there is no optical rotation component ( $\psi = 0$ ) in single scattering from this achiral spherical scatterer. The observed linear diattenuation and linear retardance originate from the difference in amplitude and phase between the scattered light polarized parallel [ $0.5 \times \{S_{11}(\Theta) + S_{12}(\Theta)\}$ ] and perpendicular [ $0.5 \times \{S_{11}(\Theta) - S_{12}(\Theta)\}$ ] to the scattering plane. The change in orientation angle of linear polarization vector of light scattered from the achiral scatterer is therefore a combined effect of linear diattenuation and linear retardance and there is no contribution of circular retardance to it. In order to unambiguously detect optical rotation introduced by the presence of chiral substances in a turbid medium (i.e., due to circular retardance property of the medium), it would be necessary to filter out the contribution of the additional rotation of polarization vector arising due to the combined effect of linear diattenuation and linear retardance. To investigate the efficacy of polar decomposition of Mueller matrix to accomplish this objective, we constructed Mueller matrix

for a chiral medium having scatterer with the same scattering parameters. The rotatory power of the chiral medium was taken to be 0.01745 radian / cm.

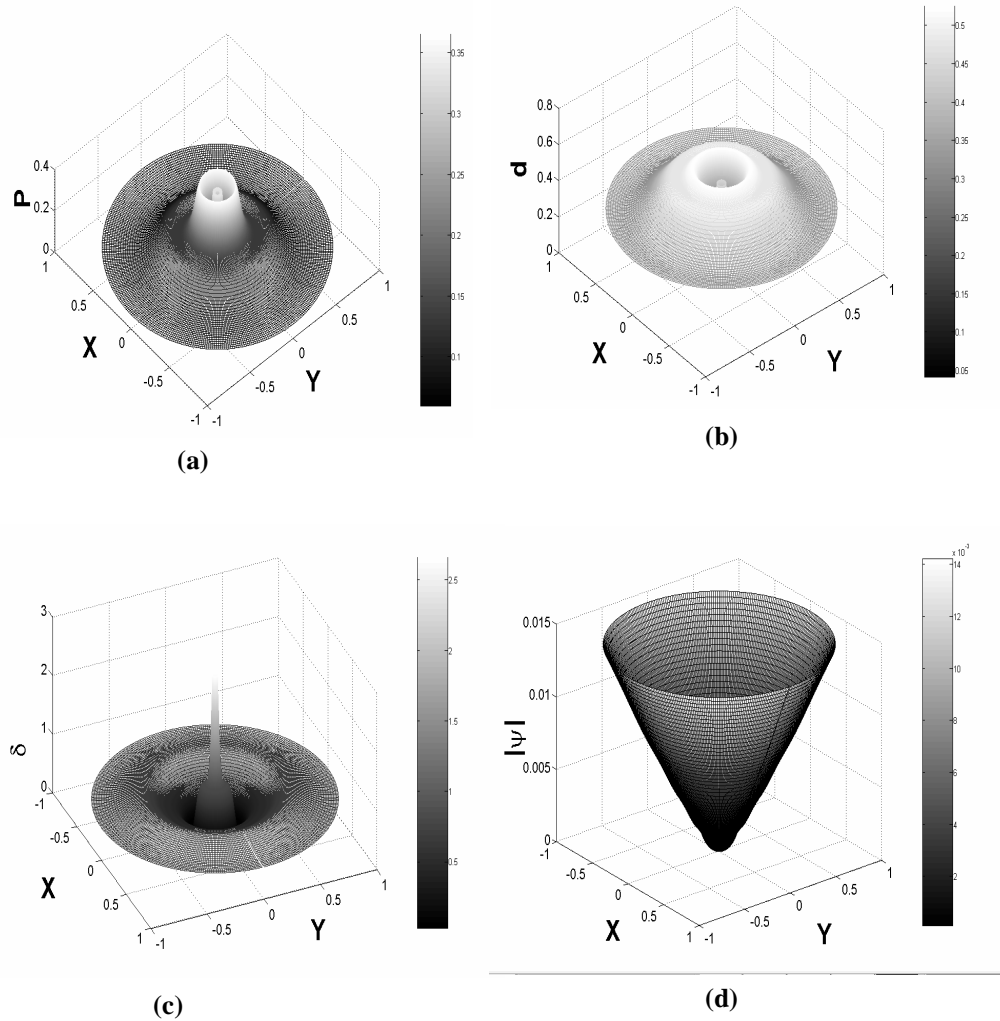


Fig. 3. (a) Depolarization (represented by degree of polarization  $P$ ) (b) diattenuation ( $d$ ), (c) linear retardance ( $\delta$ ) and (d) Optical rotation ( $\psi$ ) map of the chiral spherical scatterer obtained from polar decomposition of Mueller matrix ( $X$  and  $Y$  are in cm,  $\delta$  and  $\psi$  are in radian).

The depolarization (represented by the variation in degree of polarization  $P$ ), diattenuation ( $d$ ), linear retardance ( $\delta$ ) and optical rotation ( $\psi$ ) maps obtained using the polar decomposition process are shown in Fig. 3. As expected, the pure optical rotation ( $\psi$ ) corresponding to the chirality of the scatterer can be seen to be recovered by removing the contribution of the scattering induced linear diattenuation and linear retardance. The value for  $\psi$  is however, observed to be zero in the exact backscattering direction and increases gradually as one goes away from the point of incidence. This is expected because due to exact backscattering, the light traverses the same path twice but in opposite direction that leads to cancellation of the net optical rotation.

The theoretical results presented in this section show that the change in the orientation angle of the polarization vector of light propagating through a chiral turbid medium arises not



only due to the circular retardance property of the medium but also due to linear diattenuation and linear retardance of light scattered at large angles. Polar-decomposition of Mueller matrix can be used to decouple the contribution of linear diattenuation and linear retardance and extract the contribution of optical rotation purely due to the circular retardance property of the medium. In order to test the experimental validity of this approach, Mueller matrix measurements were performed on chiral turbid samples prepared using known concentration of scatterers and glucose molecules. The details of these studies are described in the following section.

### 3. Experimental methods

The 632.8 nm output from a He-Ne laser (Suresh Indu Lasers, India) was used as excitation source. A set of linear polarizer (P1) and a quarter wave plate (Q1) was used to illuminate the sample with desired polarization states. Another set of linear polarizer (P2) and quarter wave plate (Q2) was used to analyze the polarization states of the light scattered from the sample. The scattered light emerging from the sample was collected with an  $f/3$  lens and after passing through subsequent polarizing optics was imaged onto a CCD detector (ST6, SBIG, USA). For the measurements in the backscattering geometry, the analyzers and the collection optics were kept at an angle of  $\sim 30^\circ$  away from the exact backscattering direction. While performing measurements in the forward scattering direction, the analyzers and the collection optics were kept at an angle of  $0^\circ$  with respect to the direction of the ballistic beam. The collection angle was  $\sim 20^\circ$ .

To construct the  $4 \times 4$ -intensity measurement matrix ( $\mathbf{M}_i$ ) we generated the required four incident polarization states (linear polarization at angles of  $0^\circ$ ,  $45^\circ$ ,  $90^\circ$  from the horizontal and right circular polarization) and recorded the intensity of the light transmitted through sample after it passed through the suitably oriented analyzers (linear polarization at angles of  $0^\circ$ ,  $45^\circ$ ,  $90^\circ$  from the horizontal and right circular polarization) [26,27,28]. From this matrix the Muller matrix for the sample ( $\mathbf{M}_s$ ) was constructed using the relation [26]

$$\mathbf{M}_i = \mathbf{PSA} \mathbf{M}_s \mathbf{PSG}$$

Where, PSA and PSG are the polarization state analyzer matrix and the polarization state generator matrix respectively [26].

This kind of construction allows calibration for non-ideal components since one can replace the ideal Stokes vector in each column of PSG or each row of PSA by the measured Stoke's vectors that may deviate from ideal value. Using this approach, calibration for errors related with diattenuation and retardance of polarizer and quarter wave plate were incorporated.

The experimental set-up was calibrated by measuring Mueller matrix from known optical components such as mirror, linear polarizer and quarter wave plate. After calibration of the set-up, Mueller matrix measurements were performed on both achiral and chiral turbid samples prepared using known concentration of scatterers alone or scatterers with glucose molecules. The samples were kept inside a quartz cuvette of path length of 10 mm while taking measurements. The achiral turbid samples were prepared using aqueous suspension of polystyrene microspheres (Bangs Lab., USA) with mean diameters of  $2.0 \mu\text{m}$  (anisotropy parameter  $g = 0.91$  at 632.8 nm). The values of scattering coefficient ( $\mu_s$ ) of the samples with known concentration of microspheres were calculated using Mie theory. In order to prepare the chiral turbid samples, known concentration of D (dextro-rotatory) glucose solution was added to the microspheres suspension. The values for  $\mu_s$  of the individual chiral turbid samples were measured separately in a spectrophotometer (GBC, Cintra 20, Australia).

### 4. Results and discussion

In order to test the experimental validity of the polar decomposition based approach to decouple other polarization properties (depolarization, diattenuation and linear retardance)

from the circular retardance property for accurate determination of optical rotation, experiments were performed on samples with known retardance and optical rotation values. For this purpose, Mueller matrices were recorded in transmission mode, separately from a linear retarder (linear retardance  $\delta$  at 632.8nm  $\sim$  1.27) and from glucose solution of known concentration (5 M). Muller matrix was also recorded from the linear retarder with the glucose solution placed in front of it. Table 1(a) shows the recorded Mueller matrix ( $\mathbf{M}$ ) and the decomposed diattenuation ( $\mathbf{M}_D$ ) and retardance ( $\mathbf{M}_R$ ) matrices for the linear retarder. The value for  $\delta$  obtained using the decomposed retardance matrix  $\mathbf{M}_R$  was found to be 1.23.

Table 1. (a) Measured Mueller matrix and the decomposed components for the linear retarder.

| $\mathbf{M}$   |  |  |  |
|--|--|--|--|
| $\begin{pmatrix} 1 & -0.06 & -0.031 & 0 \\ -0.06 & 0.856 & 0.284 & -0.43 \\ -0.031 & 0.266 & 0.475 & 0.837 \\ -0.001 & 0.442 & -0.831 & 0.331 \end{pmatrix}$ |  |  |  |
| $\mathbf{M}_R$   |  | $\mathbf{M}_D$   |  |
| $\begin{pmatrix} 1 & 0 & 0 & 0 \\ 0 & 0.857 & 0.283 & -0.431 \\ 0 & 0.265 & 0.475 & 0.839 \\ 0 & 0.443 & -0.833 & 0.332 \end{pmatrix}$                       |  | $\begin{pmatrix} 1 & -0.06 & -0.031 & 0 \\ -0.06 & 1 & 0.001 & 0 \\ -0.031 & 0.001 & 1 & 0 \\ 0 & 0 & 0 & 0.998 \end{pmatrix}$ |  |

The optical rotation from the pure glucose solution kept in a 10 mm cuvette was determined to be  $\psi = 0.064$  radian (Mueller matrix not shown here). In Table 1b, we show the recorded Mueller matrix and the decomposed matrices  $\mathbf{M}_D$  and  $\mathbf{M}_R$  for the combination of the linear retarder and glucose solution. Using the matrix  $\mathbf{M}_R$  and following the procedure described in section 2.1, the values for the linear retardance and optical rotation were obtained to be  $\delta = 1.16$  and  $\psi = 0.068$  radian respectively. These values are reasonably close to the corresponding values for  $\delta$  and  $\psi$  of the linear retarder and pure glucose solution obtained from separate measurements ( $\delta = 1.23$ ,  $\psi = 0.064$  radian).

Table 1. (b) Measured Mueller matrix and the decomposed components for the combination of the linear retarder and glucose (5M) solution.

|   |  |  |  |
|---|--|--|--|
| $\mathbf{M} \begin{pmatrix} 1 & 0.09 & -0.093 & -0.2 \\ 0.155 & 0.874 & 0.119 & -0.435 \\ -0.179 & 0.303 & 0.487 & 0.804 \\ 0.029 & 0.310 & -0.837 & 0.383 \end{pmatrix}$ |  |  |  |
| $\mathbf{M}_R \begin{pmatrix} 1 & 0 & 0 & 0 \\ 0 & 0.892 & 0.130 & -0.432 \\ 0 & 0.32 & 0.492 & 0.809 \\ 0 & 0.318 & -0.861 & 0.398 \end{pmatrix}$                        |  | $\mathbf{M}_D \begin{pmatrix} 1 & 0.09 & -0.09 & -0.2 \\ 0.09 & 0.975 & -0.004 & -0.009 \\ -0.093 & -0.004 & 0.976 & 0.009 \\ -0.2 & -0.009 & 0.009 & 0.992 \end{pmatrix}$ |  |

Experiments were conducted on achiral turbid samples prepared using aqueous suspension of 2.0  $\mu\text{m}$  diameter polystyrene microspheres ( $\mu_s = 1.5 \text{ mm}^{-1}$ ,  $g = 0.91$ ) in both forward and backscattering geometry. The polar decomposition based approach could successfully decouple the scattering induced linear diattenuation and linear retardance from the measured Mueller matrix for the achiral turbid sample and yield a value of  $\psi = 0.003$  radian (data not shown here). The measured Mueller matrix ( $\mathbf{M}$ ) and the decomposed diattenuation ( $\mathbf{M}_D$ ), depolarization ( $\mathbf{M}_\Delta$ ) and retardance ( $\mathbf{M}_R$ ) matrices of a chiral turbid sample (prepared using aqueous suspension of 2.0  $\mu\text{m}$  diameter polystyrene microspheres and known concentration of glucose) for forward and backscattering geometry are displayed in Table 2(a) and 2(b) respectively. The concentration of glucose in the sample was 5M. The value for  $\mu_s$  of this chiral turbid sample was determined to be  $\mu_s = 0.6 \text{ mm}^{-1}$ . The values for the parameters, linear diattenuation ( $d$ ), linear retardance ( $\delta$ ), optical rotation ( $\psi$ ) and degree of linear polarization [defined here as  $P_L = (Q^2 + U^2)^{1/2} / I$ ] for this sample are summarized in Table 3.

Table 2. (a) Measured Mueller matrix and the decomposed components for the chiral turbid sample ( $\mu_s = 0.6 \text{ mm}^{-1}$ , glucose 5M) in forward scattering geometry

|   |  |   |  |
|---|--|---|--|
| $\mathbf{M} \begin{pmatrix} 1 & 0.026 & 0.044 & -0.039 \\ 0.029 & 0.962 & -0.144 & -0.047 \\ 0.002 & 0.126 & 0.975 & 0.026 \\ -0.039 & 0.019 & 0.115 & 0.936 \end{pmatrix}$ |  |   |  |
| $\mathbf{M}_\Delta \begin{pmatrix} 1 & 0 & 0 & 0 \\ 0.008 & 0.976 & -0.01 & -0.021 \\ -0.023 & -0.01 & 0.982 & 0.073 \\ -0.009 & -0.022 & 0.073 & 0.941 \end{pmatrix}$      | $\mathbf{M}_R \begin{pmatrix} 1 & 0 & 0 & 0 \\ 0 & 0.99 & -0.138 & -0.027 \\ 0 & 0.136 & 0.99 & -0.048 \\ 0 & 0.033 & 0.044 & 0.998 \end{pmatrix}$ | $\mathbf{M}_D \begin{pmatrix} 1 & 0.026 & 0.044 & -0.039 \\ 0.026 & 0.998 & 0.001 & -0.001 \\ 0.044 & 0.001 & 0.999 & -0.001 \\ -0.039 & -0.001 & -0.001 & 0.999 \end{pmatrix}$ |  |

Table 2. (b) Measured Mueller matrix and the decomposed components for the chiral turbid sample ( $\mu_s = 0.6 \text{ mm}^{-1}$ , glucose 5M) in backscattering geometry.

| <b>M</b>   |  |  |  |  |  |  |  |  |  |  |  |  |  |  |  |
|--|--|--|--|--|--|--|--|--|--|--|--|--|--|--|--|
| $\begin{pmatrix} 1 & -0.115 & -0.066 & 0.023 \\ -0.111 & 0.759 & -0.061 & -0.001 \\ -0.018 & 0.151 & -0.435 & -0.139 \\ -0.046 & 0.006 & 0.128 & -0.334 \end{pmatrix}$ |  |  |  |  |  |  |  |  |  |  |  |  |  |  |  |
| <b>M<sub>A</sub></b>   |  |  |  | <b>M<sub>R</sub></b>   |  |  |  | <b>M<sub>D</sub></b>   |  |  |  |  |  |  |  |
| $\begin{pmatrix} 1 & 0 & 0 & 0 \\ -0.028 & 0.756 & -0.072 & 0.021 \\ -0.062 & -0.072 & 0.488 & -0.014 \\ -0.03 & 0.021 & -0.014 & 0.358 \end{pmatrix}$                 |  |  |  | $\begin{pmatrix} 1 & 0 & 0 & 0 \\ 0 & 0.985 & -0.184 & 0 \\ 0 & -0.175 & -0.924 & -0.312 \\ 0 & 0.057 & 0.306 & -0.95 \end{pmatrix}$ |  |  |  | $\begin{pmatrix} 1 & -0.115 & -0.066 & 0.023 \\ -0.115 & 0.998 & 0.004 & -0.001 \\ -0.066 & 0.004 & 0.993 & -0.001 \\ 0.023 & -0.001 & -0.001 & 0.991 \end{pmatrix}$ |  |  |  |  |  |  |  |

Table 3. Comparison between the different polarization parameters for the chiral turbid sample ( $\mu_s = 0.6 \text{ mm}^{-1}$ , glucose 5M) in forward and backscattering geometry.

| Parameters | Forward scattering | Backscattering |
|------------|--------------------|----------------|
| d          | 0.064              | 0.135          |
| $\delta$   | 0.055              | 2.82           |
| $\psi$     | 0.069              | 0.073          |
| $P_L$      | 0.976              | 0.636          |

As expected, the values for d and  $\delta$  are observed to be larger in the backscattering geometry as compared to that obtained in the forward scattering geometry. The values for optical rotation  $\psi$  determined using the polar decomposition of Mueller matrix for both forward and backscattering geometry are slightly larger than the corresponding value for clear solution of glucose ( $\psi = 0.064$  radian) having the same concentration. This arises due to the increased path length of light in the medium due to multiple scattering [14,18,22]. It is interesting to note that the value for  $\psi$  is marginally higher in the backscattering geometry as compared to that obtained for forward scattering geometry. A plausible reason for this is the fact that for this forward scattering sample ( $g = 0.91$ ), the incident photons have to suffer significantly larger number of forward scattering events and hence have to traverse a longer path in the medium to come out from the medium through the backward direction as compared to that required for emerging through the forward direction. This would be the case if there is significant contribution of multiply scattered photons to the detected light in the backscattering geometry. Unlike the case for exact backscattering (scattering angle  $\Theta = 3.14$  radian), in this situation, the net optical rotation is not expected to cancel out, would rather add up to yield a larger value of  $\psi$  in the backscattering geometry. The fact that the value for  $P_L$  obtained from the pure depolarizing matrix is considerably lower in the backscattering direction as compared to that obtained for the forward scattering direction, suggests that this

might be the case here. This aspect is being investigated in more details by carrying out systematic studies on chiral scattering samples having different values of  $\mu_s$  and  $g$ .

In Table 4, we present the results for another chiral turbid sample with relatively larger value of  $\mu_s (= 5 \text{ mm}^{-1})$ . The value for  $\psi$  recovered after polar decomposition of Mueller matrix detected in forward geometry was found to be  $\psi = 0.076$  radian. This value of  $\psi$  is about 10 % higher than the corresponding value obtained from the turbid sample with  $\mu_s = 0.6 \text{ mm}^{-1}$  and is about 18 % higher than that obtained from the clear solution of glucose with the same concentration (5M). As noted earlier, this gradual increase of the value of  $\psi$  with increasing value of  $\mu_s$  of the chiral scattering sample arises due to the increase in path length of photons due to increased degree of multiple scattering of light in the medium. For the same reason, the value for  $P_L$  for this sample was also found to be lower ( $P_L = 0.249$ ) as compared to that obtained for the sample with  $\mu_s = 0.6 \text{ mm}^{-1}$ .

Table 4. Measured Mueller matrix and the decomposed components for the chiral turbid sample ( $\mu_s = 5 \text{ mm}^{-1}$ , glucose 5M) in forward scattering geometry.

| M   |  |  |  |   |  |  |  |  |  |  |  |  |  |  |  |
|---|--|--|--|---|--|--|--|--|--|--|--|--|--|--|--|
| $\begin{pmatrix} 1 & -0.009 & -0.021 & -0.041 \\ -0.002 & 0.256 & -0.029 & -0.003 \\ 0.024 & 0.045 & 0.235 & -0.032 \\ 0.041 & 0.024 & 0.017 & 0.538 \end{pmatrix}$ |  |  |  |   |  |  |  |  |  |  |  |  |  |  |  |
| M <sub>Δ</sub>  |  |  |  | M <sub>R</sub>  |  |  |  | M <sub>D</sub>   |  |  |  |  |  |  |  |
| $\begin{pmatrix} 1 & 0 & 0 & 0 \\ -0.001 & 0.258 & 0.01 & 0.009 \\ 0.028 & 0.01 & 0.241 & -0.015 \\ 0.064 & 0.009 & -0.015 & 0.541 \end{pmatrix}$                   |  |  |  | $\begin{pmatrix} 1 & 0 & 0 & 0 \\ 0 & 0.988 & -0.152 & -0.022 \\ 0 & 0.151 & 0.986 & -0.067 \\ 0 & 0.032 & 0.063 & 0.998 \end{pmatrix}$ |  |  |  | $\begin{pmatrix} 1 & -0.009 & -0.021 & -0.041 \\ -0.009 & 0.999 & 0 & 0 \\ -0.021 & 0 & 0.999 & 0 \\ -0.041 & 0 & 0 & 1 \end{pmatrix}$ |  |  |  |  |  |  |  |

## 5. Conclusion

To conclude, the results of our studies show that the ambiguity in the cause of the change in the orientation angle of the polarization vector of light propagating through a chiral turbid medium can be lifted with full Mueller matrix measurements. Polar decomposition of Mueller matrix can then be used to extract the component of optical rotation arising purely due to the circular retardance property (introduced by the presence of chiral molecules) of the medium from the other causes (linear diattenuation and linear retardance) of optical rotation. The validity of this approach was tested by conducting studies on chiral turbid samples prepared using known concentration of scatterers and glucose molecules. This approach may therefore facilitate determination of the concentration of chiral substances present in a medium using the measured Mueller matrix from the medium in both forward and backscattering geometry.